

- inflammatory response triggered by dying cells. *Nat Med.* **13**, 851-856 (2007)
- 36 Hirotsu S, *et al.* Crystal structure of a multifunctional 2-Cys peroxiredoxin heme-binding protein 23kDa/proliferation-associated gene product. *Proc Natl Acad Sci U S A.* **96**, 12333-12338 (1999)
- 37 Declercq JP, *et al.* Crystal structure of human peroxiredoxin 5, a novel type of mammalian peroxiredoxin at 1.5 Å resolution. *J Mol Biol.* **311**, 751-759 (2001)
- 38 Choi HJ, *et al.* Crystal structure of a novel human peroxidase enzyme at 2.0 Å resolution. *Nat Struct Biol.* **5**, 400-406 (1998)
- 39 Chen GY, Nuñez G. Sterile inflammation: sensing and reacting to damage. *Nat Rev Immunol.* **10**, 826-837 (2010)
- 40 Yu M, *et al.* HMGB1 signals through toll-like receptor (TLR) 4 and TLR2. *Shock.* **26**, 174-179 (2006)
- 41 Triantafilou M, *et al.* Membrane sorting of toll-like receptor (TLR)-2/6 and TLR2/1 heterodimers at the cell surface determines heterotypic associations with CD36 and intracellular targeting. *J Biol Chem.* **281**, 31002-31011 (2006)
- 42 Yi H, *et al.* Pattern recognition scavenger receptor SRA/CD204 down-regulates Toll-like receptor 4 signaling-dependent CD8 T-cell activation. *Blood.* **113**, 5819-5828 (2009)
- 43 Akashi-Takamura S, Miyake K. TLR accessory molecules. *Curr Opin Immunol.* **20**, 420-425 (2008)
- 44 Eismann T, *et al.* Peroxiredoxin-6 protects against mitochondrial dysfunction and liver injury during ischemia-reperfusion in mice. *Am J Physiol Gastrointest Liver Physiol.* **296**, G266-274 (2009)
- 45 Liu K, *et al.* Anti-high mobility group box 1 monoclonal antibody ameliorates brain infarction induced by transient ischemia in rats. *FASEB J.* **21**, 3904-3916 (2007)
- 46 Qiu J, *et al.* Early release of HMGB-1 from neurons after the onset of brain

ischemia. *J Cereb Blood Flow Metab.* **28**, 927-938 (2008)

47 Sugimori H *et al.* Krypton laser-induced photothrombotic distal middle cerebral artery occlusion without craniectomy in mice. *Brain Res Protoc.* **13**, 189-196 (2004)

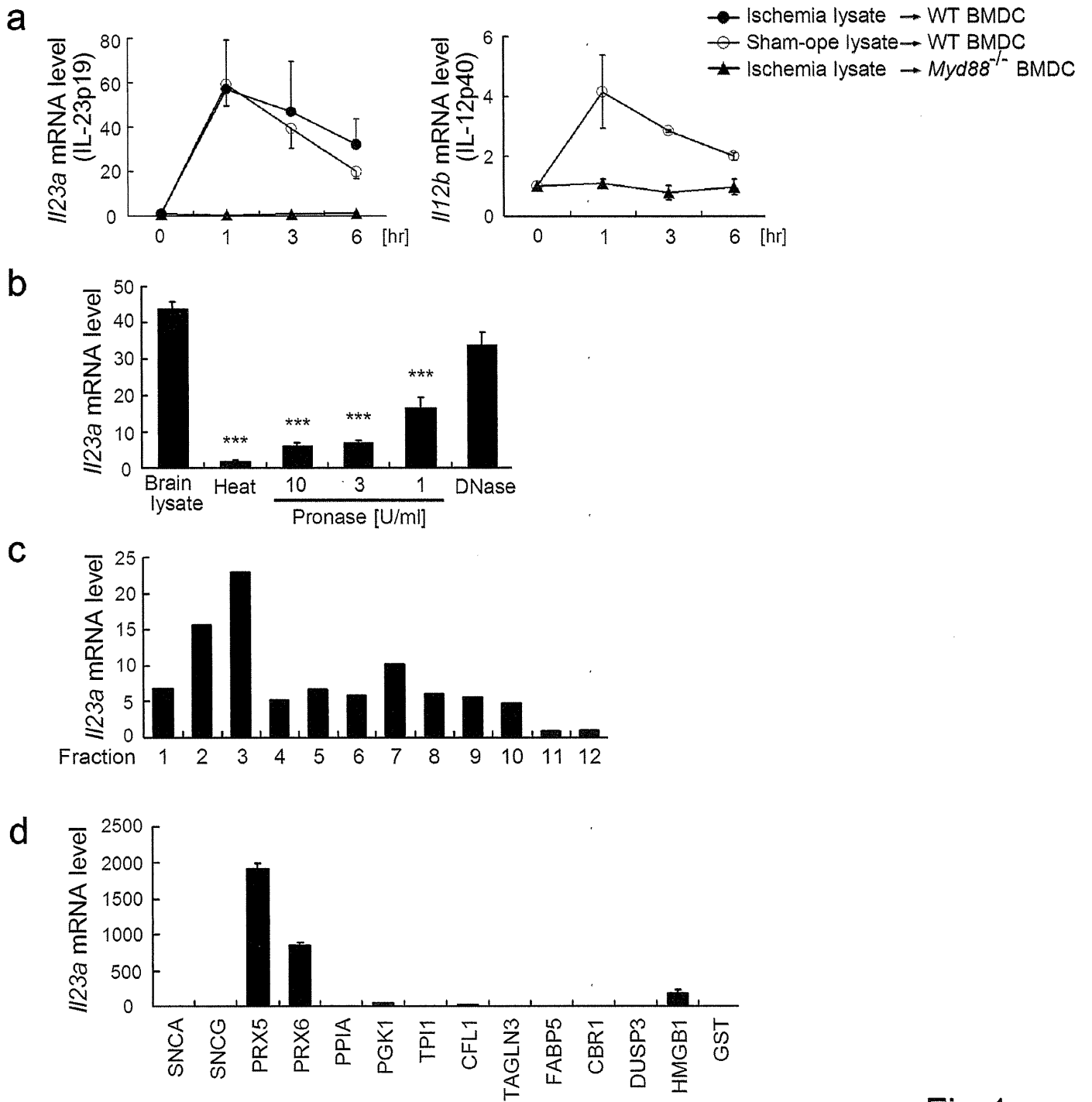


Fig.1

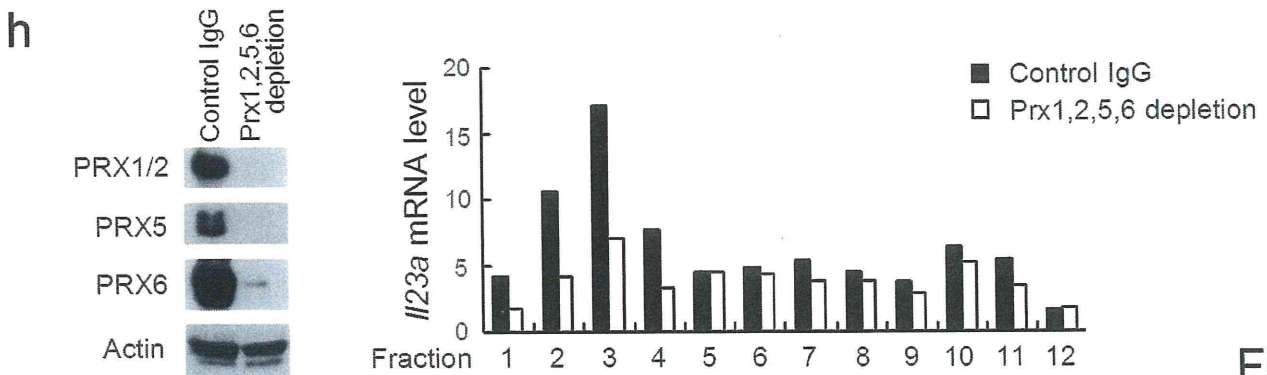
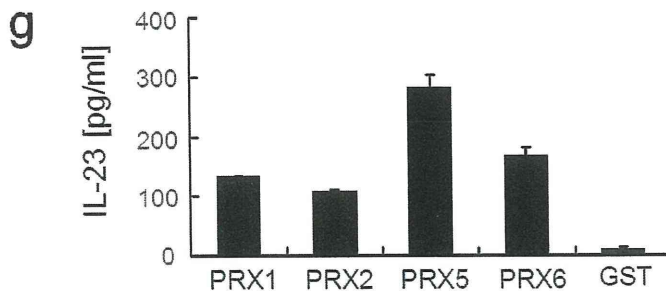
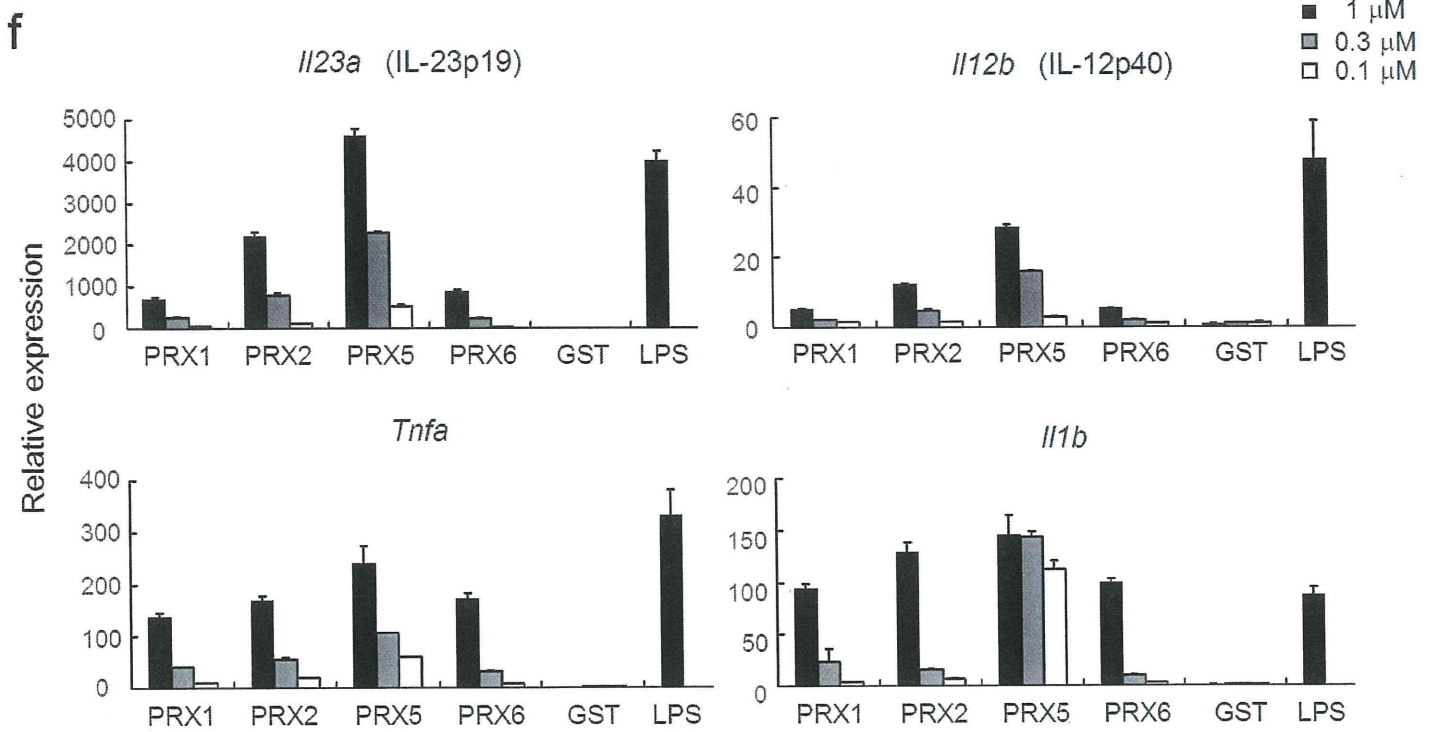
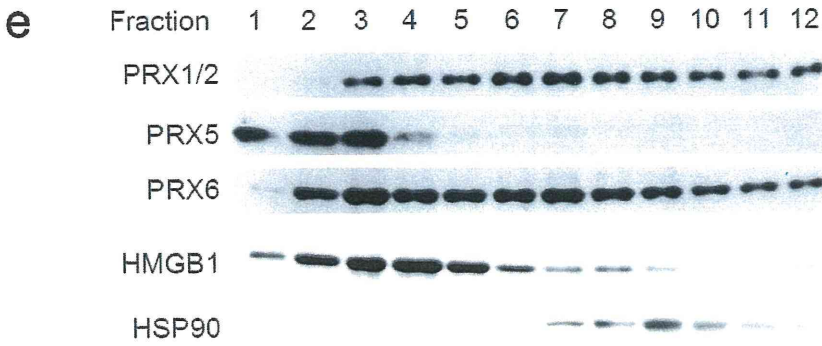


Fig.1

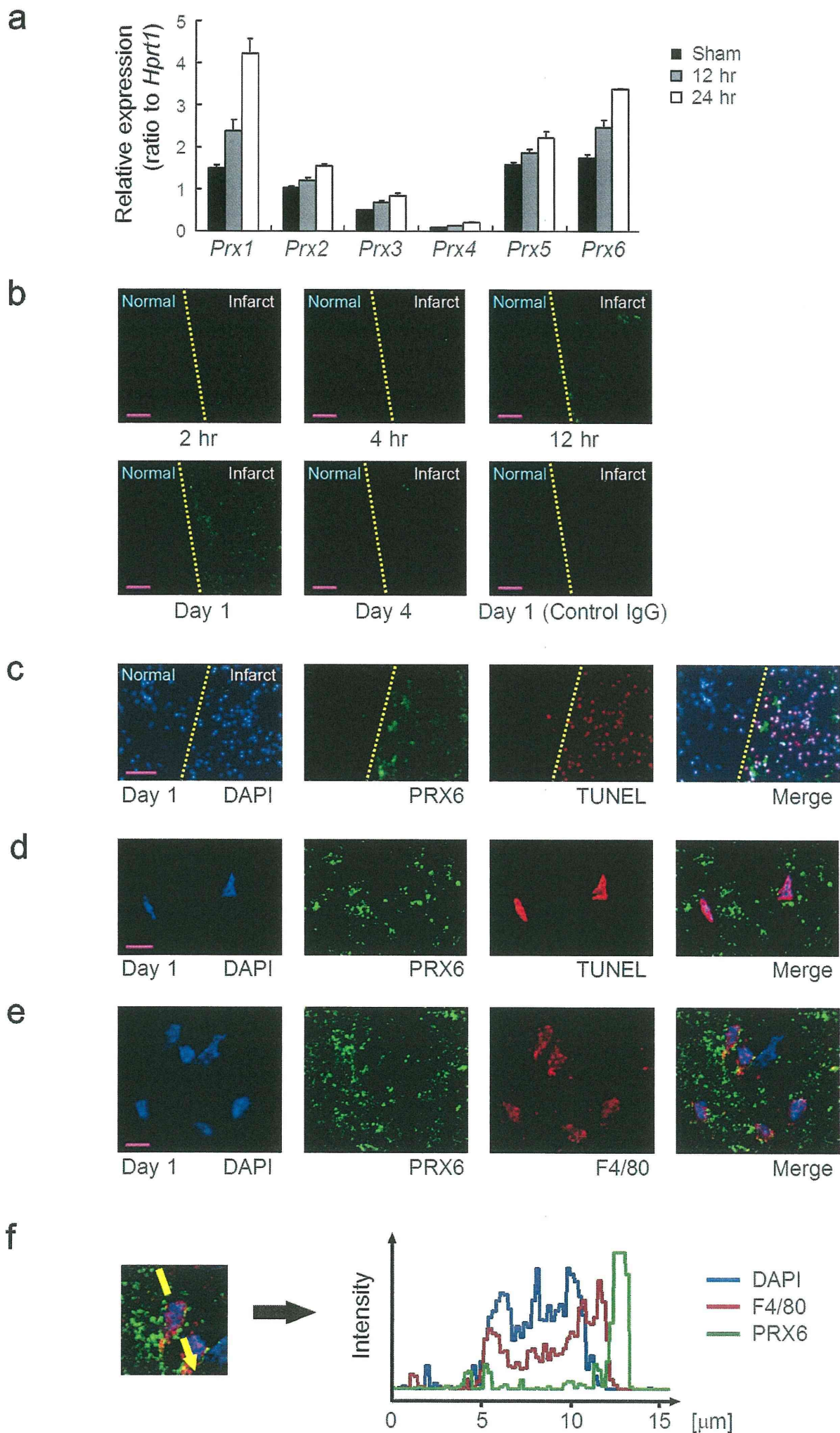


Fig.2

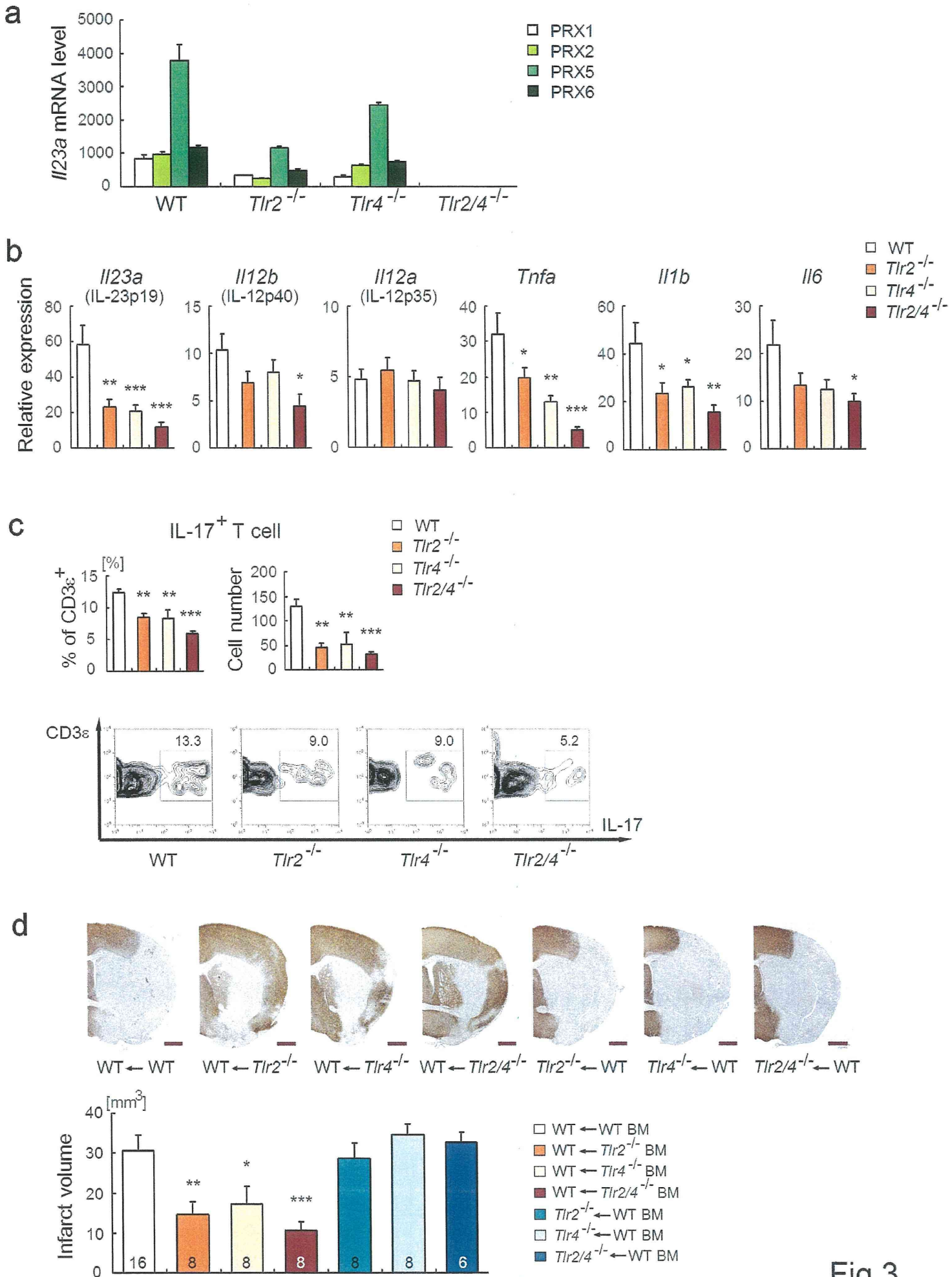


Fig.3

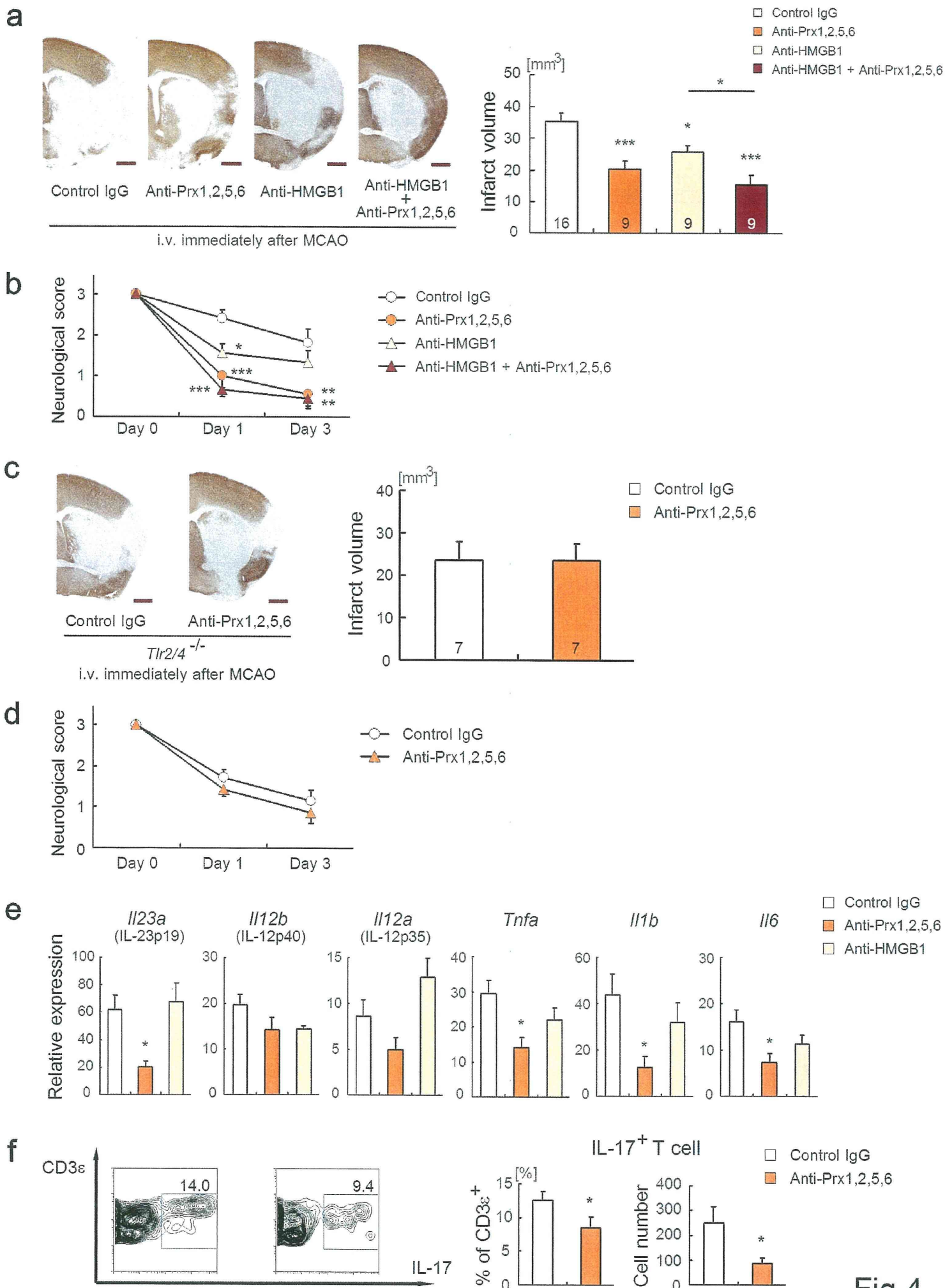


Fig.4

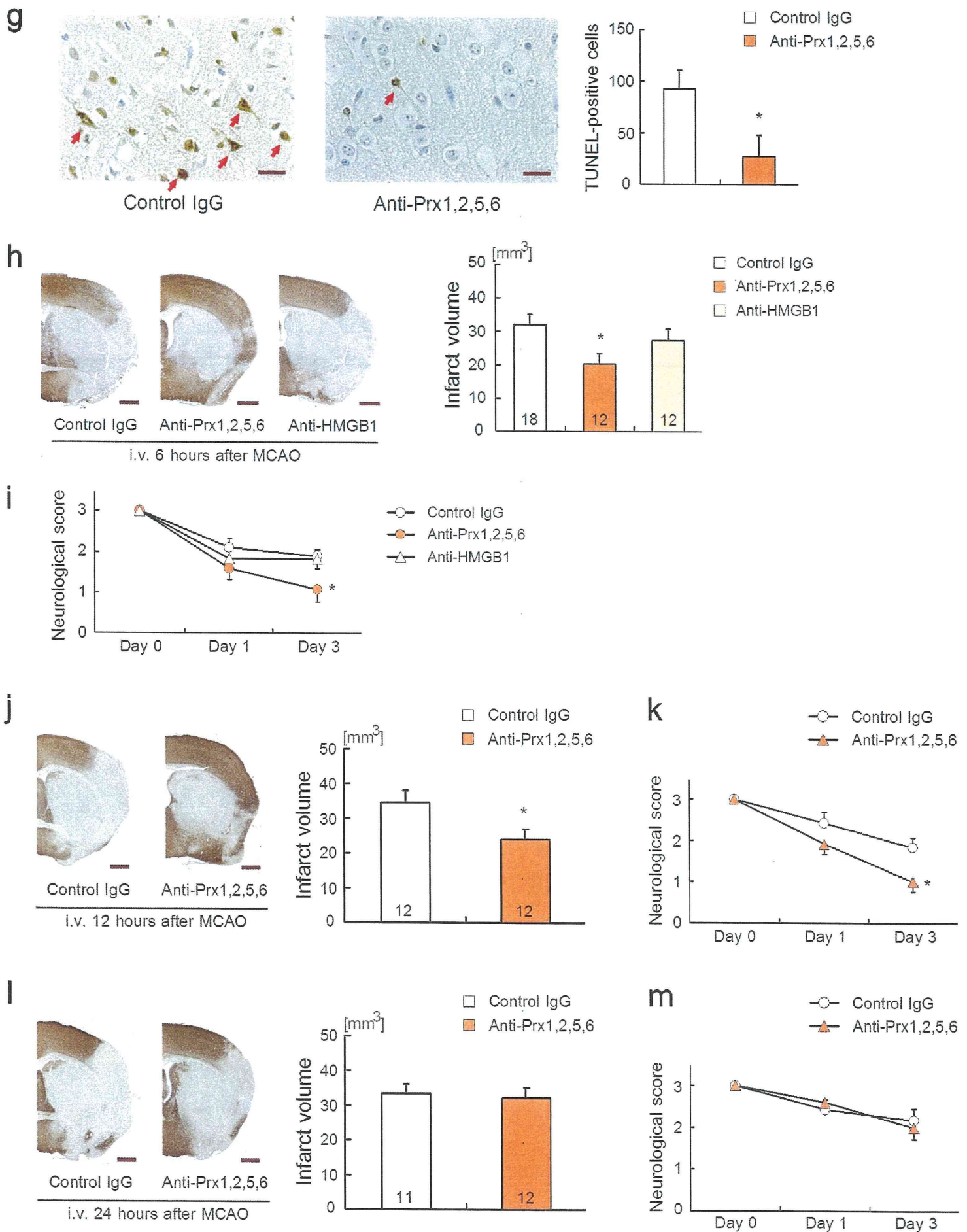


Fig.4

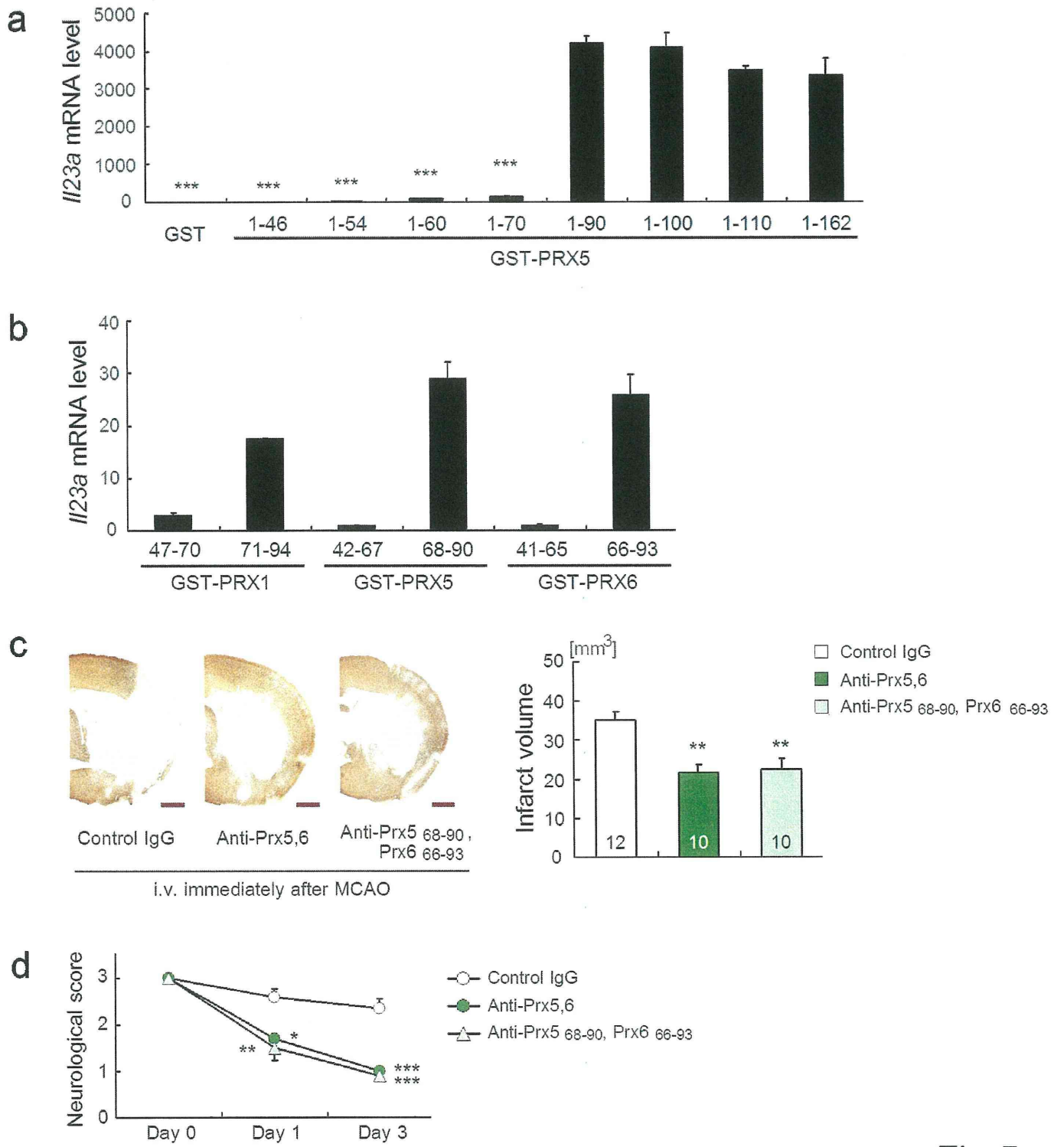
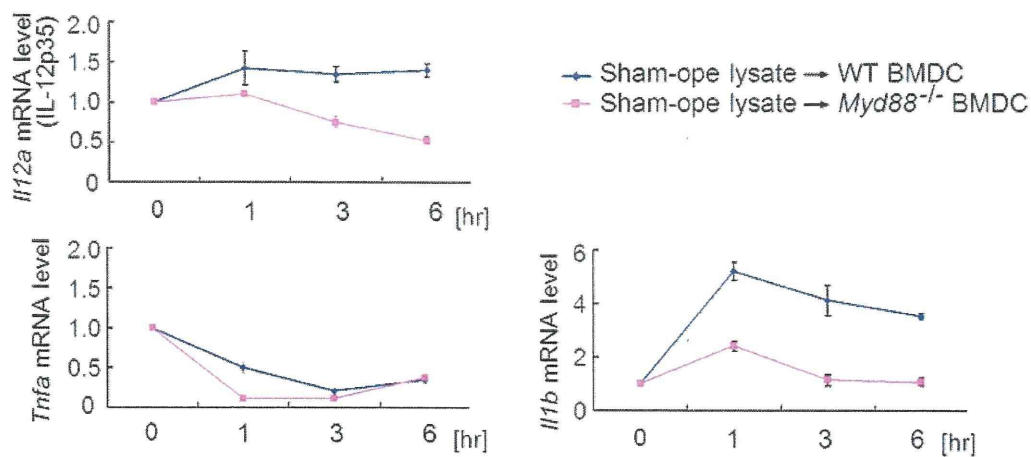


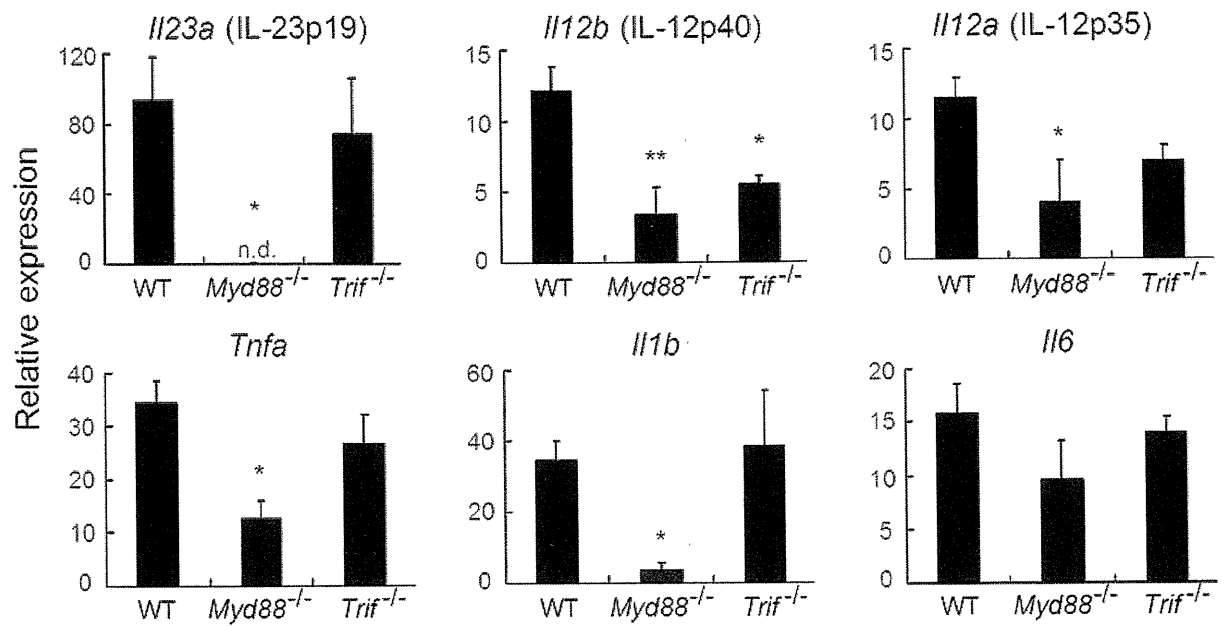
Fig.5

Peroxiredoxin family proteins are key initiators of post-ischemic inflammation in the brain

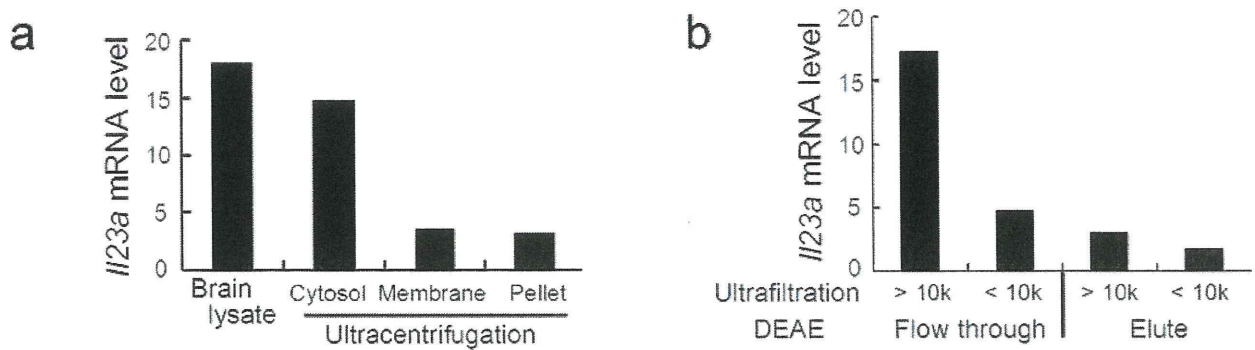
Takashi Shichita, Eiichi Hasegawa, Akihiro Kimura, Rimpei Morita, Ichiro Takada, Takashi Sekiya, Hiroaki Ooboshi, Takanari Kitazono, Toru Yanagawa, Tetsuro Ishii, Hideo Takahashi, Shuji Mori, Masahiro Nishibori, Kazumichi Kuroda, Kensuke Miyake, Shizuo Akira, and Akihiko Yoshimura



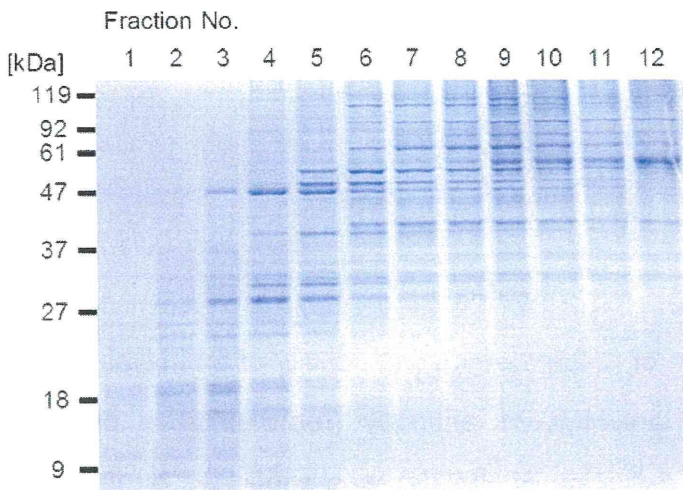
Supplementary Figure 1. The time course of IL-12p35, TNF- α , and IL-1 β mRNA expression levels in WT and *Myd88*^{-/-} BMDC induced by the addition of sham-operated brain lysate ($n = 3$, each).



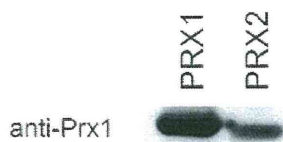
Supplementary Figure 2. The mRNA expression levels of inflammatory cytokines in the infiltrating immune cell in the ischemic brain on day 1. WT, $n = 5$; *Myd88*^{-/-} and *Trif*^{-/-}, $n = 3$. * $p < 0.05$, ** $p < 0.01$ vs. wild-type [one-way ANOVA with Dunnett's correction; error bars represent s.e.]. n.d.: not detected.



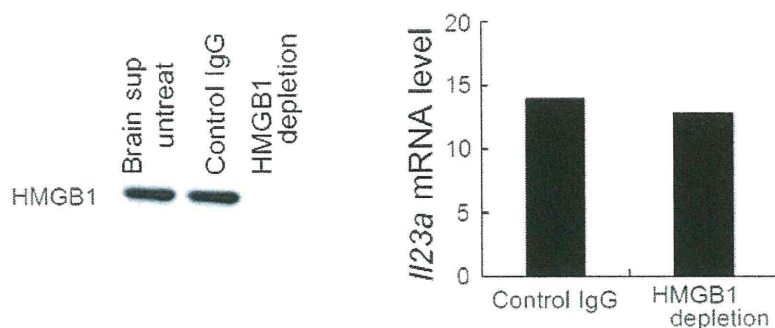
Supplementary Figure 3. (a) The IL-23p19 mRNA expression levels in BMDC 1 hour after the stimulation by each fraction of ultracentrifugation. (b) The IL-23p19-inducing activity of each fraction by ultrafiltration (10 kDa cut-off) and DEAE Sepharose (representative data of three independent experiments).



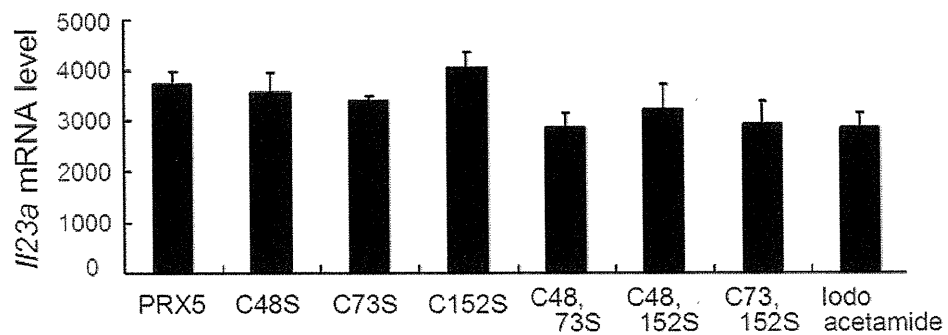
Supplementary Figure 4. SDS-PAGE analysis with CBB staining of each sucrose gradient fraction of the brain lysate (representative data of five independent experiments).



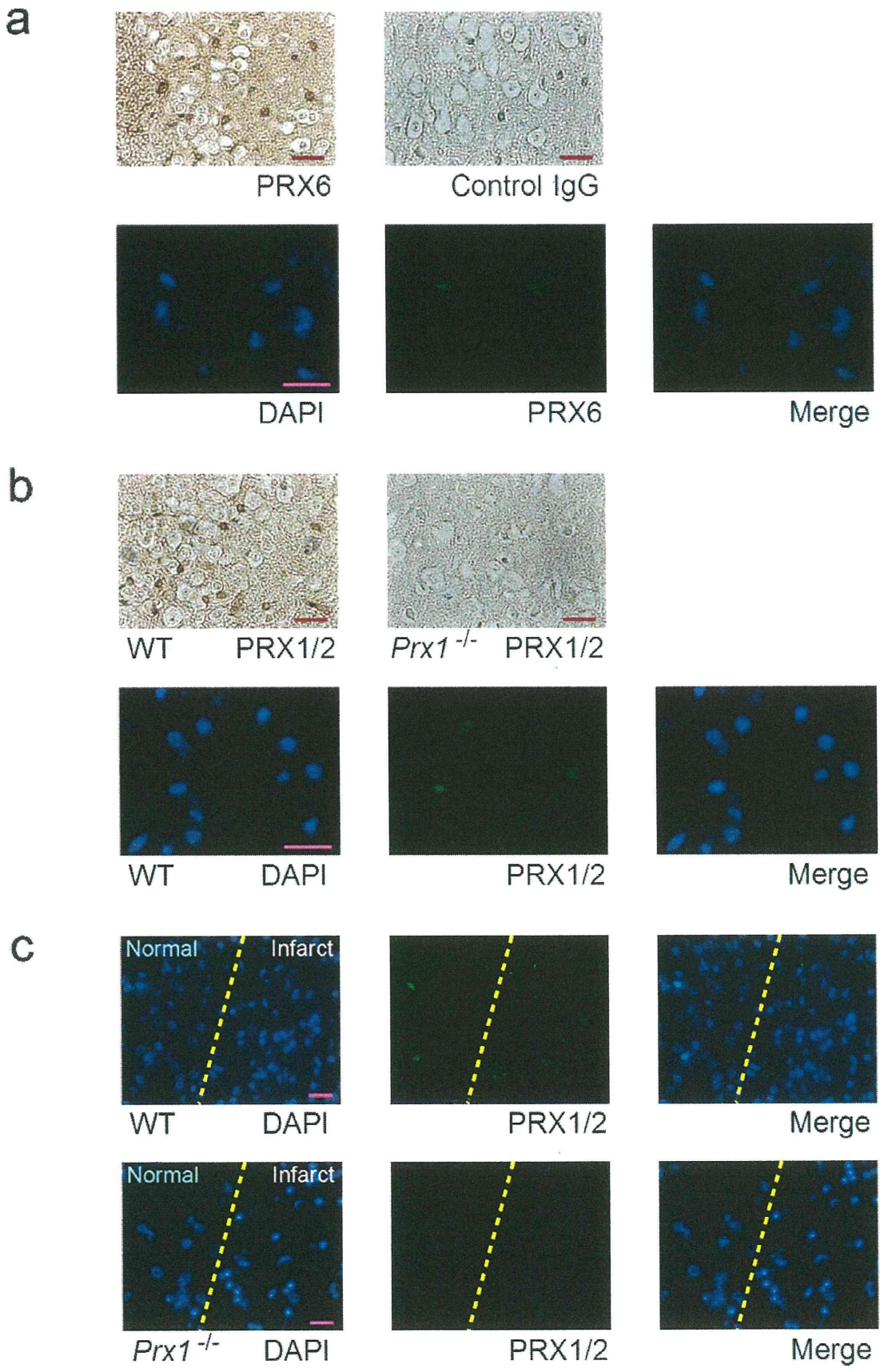
Supplementary Figure 5. Western blot analysis using rabbit polyclonal anti-Prx1 antibody. Due to the high homology between Prx1 and Prx2, anti-Prx1 antibody could also detect Prx2.



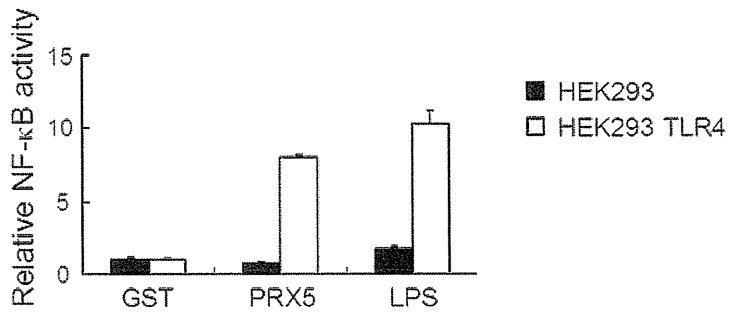
Supplementary Figure 6. The comparison of IL-23p19-inducing activity of brain lysate after the immunoprecipitation with control IgG or anti-HMGB1 antibody (representative data of two independent experiments). The complete depletion of HMGB1 was confirmed by Western blot analysis.



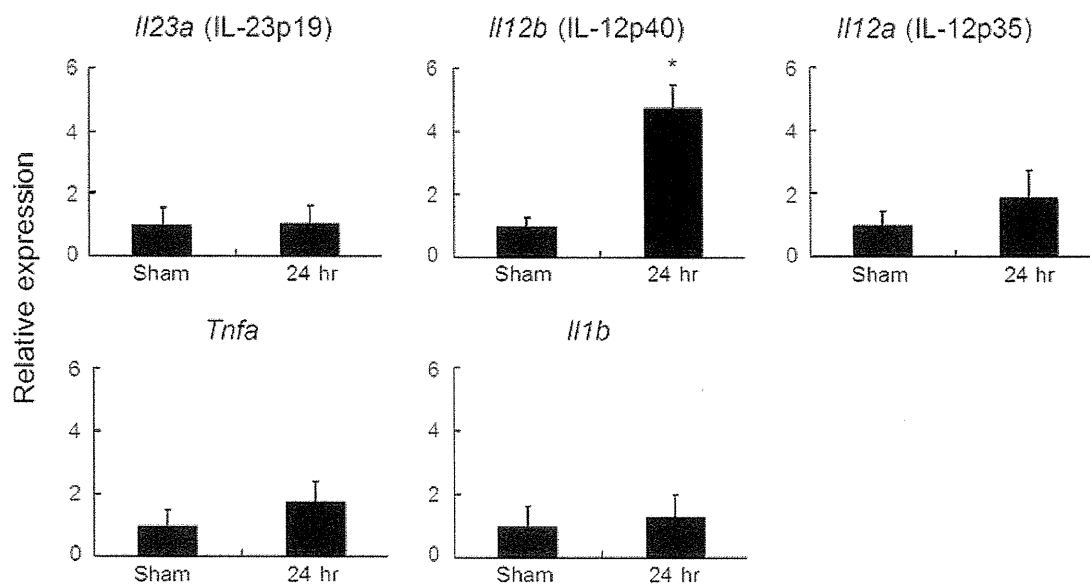
Supplementary Figure 7. The IL-23p19-inducing activity of point-mutated PRX5 protein and alkylated PRX5 protein by iodoacetamide in BMDC ($n = 3$, each).



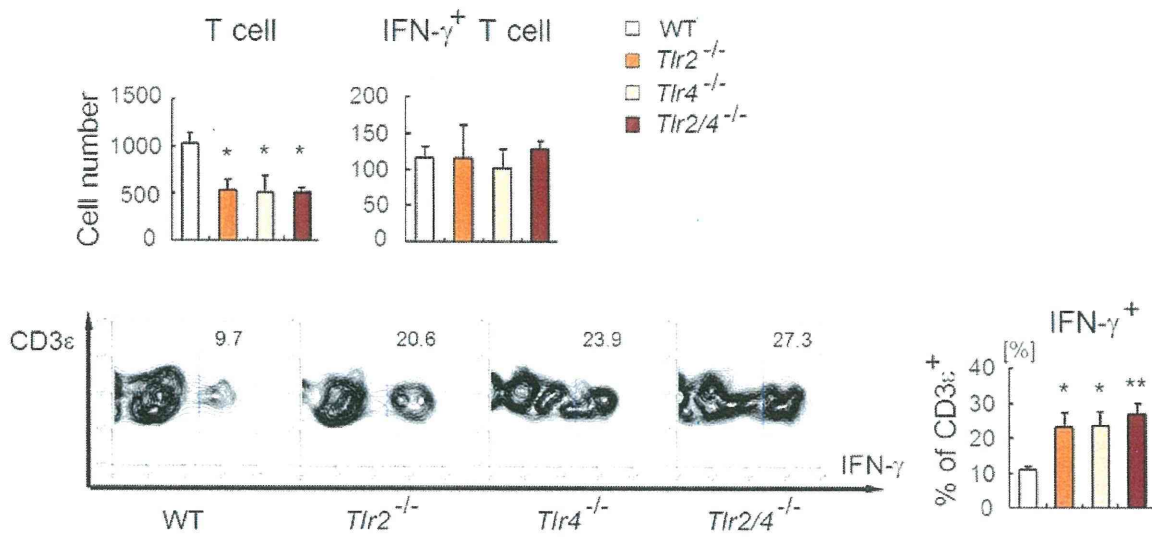
Supplementary Figure 8. (a) Anti-Prx6 immunohistostaining of normal brain tissue detected by DAB (upper panel) or Alexa Fluor 488 (lower panel). Control IgG was used for negative control. The pattern of anti-Prx6 immunostaining was similar to previous report¹. We could find anti-Prx6 positive cells by high sensitivity imaging (lower panel), although this fluorescence intensity was weak compared to Prx6-positive debris (**Fig.2b**) (bar: 20 μ m). (b) Anti-Prx1/2 immunohistostaining of normal brain tissue detected by DAB (upper panel) or Alexa Fluor 488 (lower panel). (bar: 20 μ m) (c) Anti-Prx1/2 immunohistostaining of day 1 ischemic brain tissue detected by Alexa Fluor 488. (bar: 20 μ m)



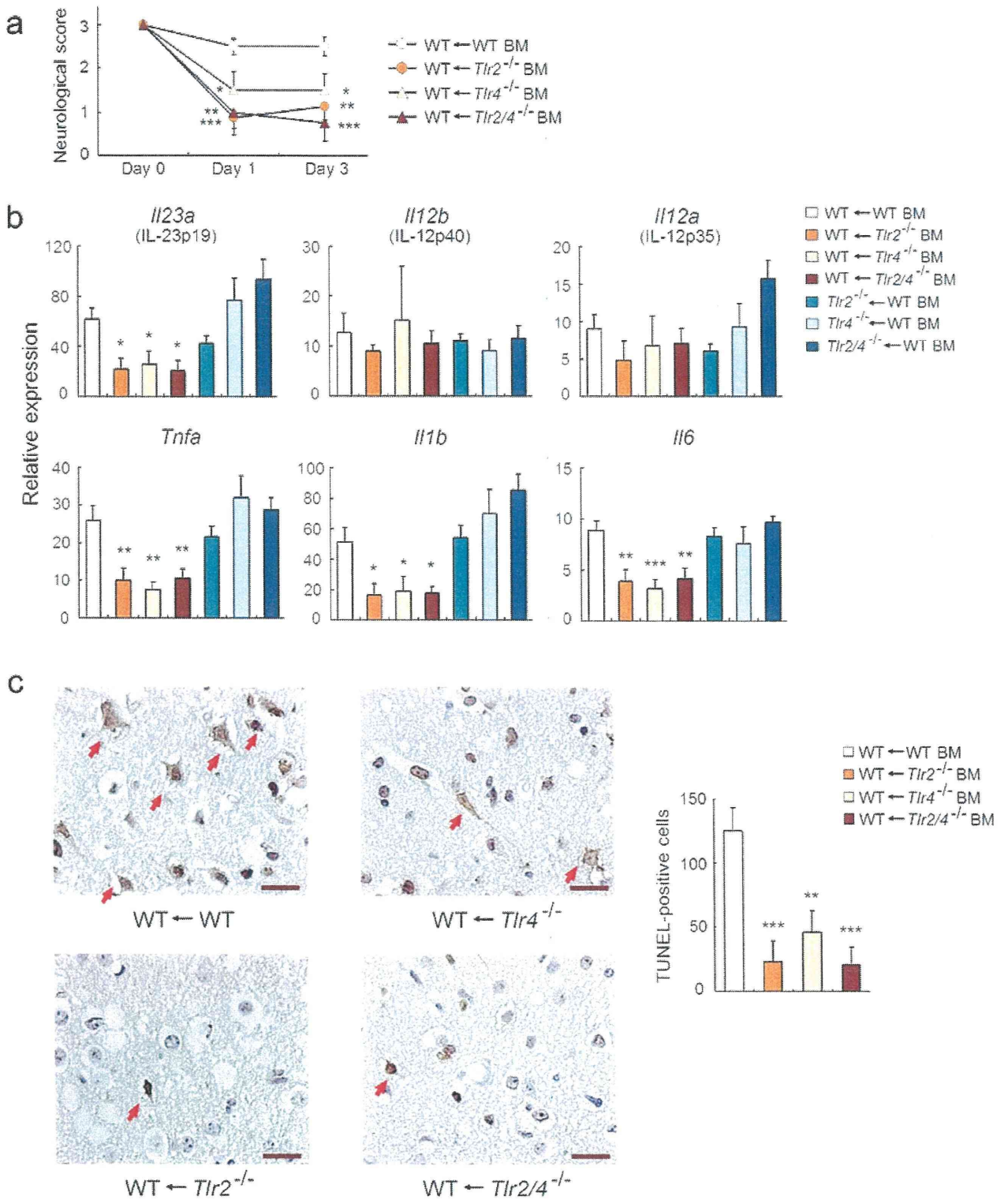
Supplementary Figure 9. The relative NF-κB activity in HEK293 or HEK293 TLR4 cell line by NF-κB luciferase assay 1 hour after stimulation by GST or PRX5 protein (1 μ M) or LPS (100 ng ml^{-1}).



Supplementary Figure 10. The mRNA expression levels of inflammatory cytokines in peripheral blood monocytes of sham-operated mice or mice 24 hours after the induction of brain ischemia ($n = 3$ for each). * $p < 0.05$ vs. Sham [two-sided Student's t -test; error bars represent s.e.].



Supplementary Figure 11. The absolute number and the ratio of IFN- γ ⁺ T cell on day 3 ($n = 8$ for WT and $n = 6$ for other samples). TLR2 and/or TLR4 deficiency significantly increased the ratio of IFN- γ ⁺ T cells, because the number of IFN- γ ⁺ T cells was kept in spite of decreased number of total infiltrating T cells. * $p < 0.05$, ** $p < 0.01$ vs WT (one-way ANOVA with Dunnett's correction; the error bars represent s.e.).



Supplementary Figure 12. (a) Neurological scores of WT or TLR-KO BM chimeric mice on days 1 and 3. (b) The mRNA expression levels of inflammatory cytokines in the infiltrating immune cells of WT or TLR-KO BM chimeric mice on day 1. (c) The results of TUNEL staining of the